Soil & Tillage Research 208 (2021) 104902

Contents lists available at ScienceDirect

Soil & Tillage Research

journal homepage: www.elsevier.com/locate/still

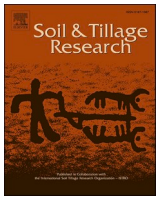

PM2.5 and PM10 emissions by breakage during saltation of agricultural soils

John Tatarko [a,*], Matthew Kucharski [b], Hongli Li [c], Huiru Li [d]

[a] USDA-ARS Rangeland Resources and Systems Research Unit, Fort Collins, CO, United States
[b] Former USDA-ARS Agricultural Systems Research Unit, Manhattan, KS, United States
[c] Forestry College of Shandong Agricultural University and Mountain Tai Forest Ecosystem Research Station of State Forestry and Grassland Administration, Tai'an, Shandong, China
[d] State Key Laboratory of Earth Surface Processes and Resource Ecology, Faculty of Geographical Science, Beijing Normal University, Beijing, China

ARTICLE INFO

Keywords:
Dust emission
PM2.5/PM10 ratio
Wind tunnel
Conventional tillage
No-till

ABSTRACT

Breakage of soil aggregates during saltation is one process that contributes to the generation of fine dust emissions by wind erosion. Fine dust is also known to affect human respiratory health. Of particular hazard are particles of aerodynamic diameter less than 2.5 μm (PM2.5) and those less than 10 μm (PM10), both of which are regulated by the US-Environmental Protection Agency. We used a laboratory wind tunnel with wind at 13 m s^{-1} to investigate the emission parameters for PM2.5 and PM10 caused by saltation-size aggregates (0.15 to 0.84 mm) from 15 soils with a wide range in properties from across the U.S. The coefficient of breakage (C_{bk}) was found to vary inversely with clay content, with the largest values found for soils with the greatest sand content. Only one soil with the highest sand content was found to be statistically different in total suspension flux from breakage (Gss_{bk}). We did not find a relationship between soil texture or organic matter and the soil fraction of PM2.5 and PM10 from breakage ($SF2.5_{bk}$ and $SF10_{bk}$). In addition, five of the soils tested had long-term histories of either conventional tillage (CT) or no-till (NT) management for paired comparisons of emission based on management. CT soils tended to have higher sand, lower silt and lower organic matter than NT management. Management significantly affected C_{bk} for four of the five soil pairs where the three with the highest clay content having lower C_{bk} under NT than CT management and the fourth pair had lower C_{bk} under CT management. Long-term NT management showed significantly less vertical suspension flux from breakage during saltation (Gss_{bk}) than CT management for only two of the five paired soils. A linear relationship predicted PM2.5 emissions from breakage as a fraction of PM10 emissions for the mineral soils tested ($R^2 = 0.972$). This research contributes to our understanding of PM2.5 and PM10 emission during saltation. It also provides parameters that will improve fine dust simulation in the Wind Erosion Prediction System (WEPS) model.

1. Introduction

Wind erosion of soil is known to affect an array of agroecosystem services including those of soil, air, and water quality (see Tatarko et al., 2019). Fine dust from wind erosion also contributes to global climate change (Lambert et al., 2008; Prospero and Lamb, 2003) and dust fall reduces albedo of mountain snow causing earlier melt, altering regional and continental hydrology (Painter et al., 2012, 2017; Chenglai et al., 2018). Blowing dust causes hazards to highway traffic representing a significant environmental, health and safety concern for transportation infrastructure in dry regions (Middleton, 2017; Li et al., 2017). Fine particulates from wind erosion are also known to be a human respiratory hazard. Particulate matter of less than 2.5 μm and 10 μm mean aerodynamic diameter, designated as PM2.5 and PM10 respectively, can penetrate deep into the lungs and affect pulmonary systems (Goudie, 2014; .Kjelgaard et al., 2004). The association between long-term exposure to PM2.5 and mortality is well documented (Dockery et al., 1993, Liu et al., 2019). The United States Environmental Protection Agency (US-EPA) established outdoor air quality standards for PM10 in 1987 at 150 μg m^{-3} of 24-h of average concentration (US-EPA, 1999). The US-EPA later regulated mass concentration for PM2.5 (US-EPA, 1996) and in 2012, set the standard for PM2.5 at 35 μg m^{-3} for 24 h (US

* Corresponding author at: USDA-ARS Rangeland Resources and Systems Research Unit, 2150 Centre Avenue, Bldg. D. Suite 200, Fort Collins, 80526, Colorado, United States.
E-mail address: John.Tatarko@usda.gov (J. Tatarko).

https://doi.org/10.1016/j.still.2020.104902
Received 3 September 2020; Received in revised form 24 November 2020; Accepted 26 November 2020
Available online 28 December 2020

Federal Register, 2013).

Understanding the physical processes of wind erosion and fine dust emissions is essential for developing reliable prediction methods as well as effective controls of fugitive dust. Mirzamostafa et al. (1998) identified three explicit sources of the suspension-size component of wind erosion, defined as particles < 100 μm in diameter. Those sources of suspension include: 1) direct emissions of loose material from the surface, 2) abrasion of surface crusts and aggregates (e.g., clods), and 3) breakage of saltating soil aggregates. The first two sources for PM2.5 and PM10 have been studied in a series of wind tunnel tests (Li et al., 2015 and Tatarko et al., 2020). This study investigates the third source of breakage using the same wind tunnel and soils.

The Wind Erosion Prediction System (WEPS) model, which was developed by the USDA Agricultural Research Service, simulates wind erosion soil loss from agricultural fields (Tatarko et al., 2019; Wagner, 2013). As part of the model, WEPS simulates the three sources of suspension emissions proposed by Mirzamostafa et al. (1998). The total suspension flux is equal to the sum of the individual components:

$$Gss = Gss_{en} + Gss_{an} + Gss_{bk} \quad (1)$$

where

Gss = total suspension vertical flux (kg m^{-2} s^{-1}),

Gss_{en} = vertical flux from emission of loose aggregates (kg m^{-2} s^{-1}),

Gss_{an} = vertical flux from abrasion of surface clods and crust (kg m^{-2} s^{-1}), and

Gss_{bk} = vertical flux of suspension-size from breakage of saltating aggregates (kg m^{-2} s^{-1}).

Each of the three components are calculated separately since their generation processes and transport are considered as independent processes in WEPS (Hagen and Fox, 2020). As aggregates are transported in saltation, they undergo multiple impacts and partial breakdown. This process produces suspension-size aggregates, which are assumed to be mixed thoroughly with the saltation-size and emitted with them.

The suspension-size flux from breakdown by saltation impacts is simulated in WEPS as (Mirzamostafa et al., 1998):

$$Gss_{bk} = C_{bk} * q(1 - q_s) \quad (2)$$

where

C_{bk} = coefficient of breakage (m^{-1}),

q = horizontal saltation discharge (kg m^{-1} s^{-1}), and

q_s = discharge of primary (non-breakable) sand particles (kg m^{-1} s^{-1}).

The discharge of primary sand particles, q_s, is approximated using:

$$q_s = SF_{sand} * q \quad (3)$$

where

SF_{sand} = fraction of surface soil that is sand.

Here, we define the coefficient of breakage as the soil loss from the cumulative distance traveled for each unit mass of saltation passing a unit across-wind width. Eq. 2 can be solved to provide C_{bk} according to Mirzamostafa et al. (1998):

$$C_{bk} = -\frac{1}{X} * \ln[(q - q_s)/(q_o - q_s)] \quad (4)$$

where

q_o = initial saltation discharge (kg m^{-1} s^{-1}) and

X = cumulative distance traveled by saltating aggregates (m).

The WEPS model simply assumes that PM10 is a fraction of the suspension-size aggregates broken from saltation-size aggregates ($SF10_{bk}$). Thus the PM10 flux from breakdown in WEPS was described by Mirzamostafa et al. (1998) as:

$$G10_{bk} = SF10_{bk} * Gss_{bk} \quad (5)$$

where

$G10_{bk}$ = vertical flux of PM10 from saltation breakdown (kg m^{-2} s^{-1}),

$SF10_{bk}$ = soil fraction of PM10 in suspension sized aggregates created during saltation breakdown.

A similar equation can be used to provide the PM2.5 flux from saltation breakdown (i.e., $G2.5_{bk}$) as calculated from the soil fraction of PM2.5 in suspension sized aggregates created during saltation breakdown ($SF2.5_{bk}$) and Gss_{bk}:

$$G2.5_{bk} = SF2.5_{bk} * Gss_{bk} \quad (6)$$

The WEPS model also simulates the temporal (i.e., daily) state of surface erodibility by accounting for the effects of weather and management operations such as tillage on soil water dynamics, plant growth, residue decomposition, and soil wind erodibility. Weather and management (i.e., tillage) are known to affect soil properties and aggregation in particular (Skidmore et al., 1986). Thus, a better understanding of the effects of management on aggregation and its effects on emissions can improve wind erosion models such as WEPS. Tillage has been shown to modify soil aggregate size and stability (Karlen et al., 1994; Lopez et al., 2000; Sheehy et al., 2015). Only a few studies have been reported on the effects of tillage management on wind erosion emissions (Skidmore et al., 1986; Lopez et al., 2000; Li et al., 2015; Tatarko et al., 2020).

Hagen (2004) studied breakage of saltation-size aggregates by impacting them on a steel plate in an enclosed chamber. Breakage coefficients for saltation-size aggregates have also been measured in the wind tunnel (Mirzamostafa et al., 1998), but that study only considered three soils (i.e., two silt loams, and one silty clay loam) and only reported suspension-sized emissions. Emissions of PM2.5 and PM10 from loose particles and abrasion of immobile clods in soils were previously reported for wind tunnel studies by Li et al. (2015) and Tatarko et al. (2020). However, a determination of the PM2.5 and PM10 emissions from breakage of saltating aggregates have not been made, so this research seeks to derive the parameters for breakage as a source for PM2.5 and PM10. The objectives of this study were to derive for a wide variety of soils, the coefficient of breakage (C_{bk}), the vertical flux of suspension-size from breakage of saltation-size aggregates (Gss_{bk}), and the fraction of soil in the form of PM2.5 and PM10 created during saltation breakdown ($SF2.5_{bk}$ and $SF10_{bk}$, respectively) as used in the WEPS model. A secondary objective was to compare the derived parameters for conventional tillage (CT) vs. no-till (NT) management for selected pairs of soils, to ascertain the potential effects of tillage management on emissions from breakage of saltating aggregates.

2. Methods

2.1. Wind tunnel setup and dust sampling system

Setup of the wind tunnel fan, screen, honeycomb, and spires (see Fig. 1, Nos. 1–3), as well as the tunnel dimensions (13 L × 1.20 W × 1.47 H m) remained identical to the previous PM2.5 and PM10 tests conducted in the wind tunnel by Li et al. (2015) who measured loose emissions and Tatarko et al. (2020) who measured emissions by abrasion of soil clods. Saltation-size aggregates traveled the entire 12.4 m length of the tunnel section over a bare 19 mm thick plywood floor. Wind tunnel tests by Mirzamostafa (1996) found using plywood as the wind tunnel floor does simulate field conditions in studying saltation breakdown on a soil surface. Gaps or cracks where particles could accumulate were either filled with silicone or covered with tape.

An isokinetic, vertical-slot sampler system (Fig. 1, Nos 6–12) (Mirzamostafa et al., 1998; Van Pelt et al., 2010) was located in the center of the wind tunnel width and sampled generated suspension-size dust (< 100 μm). The sampler slot had a 3.9 W × 359 H mm opening and was 11.2 m downwind from the source of saltation sized aggregates (Fig. 1, No. 4). The slot sampler system also used the same pressure transducers and computer setup as previous wind tunnel tests (Li et al., 2015; Tatarko et al., 2020). The slot sampler system included a single pump system (Fig.1, Nos. 11&12) with a Grimm portable aerosol spectrometer

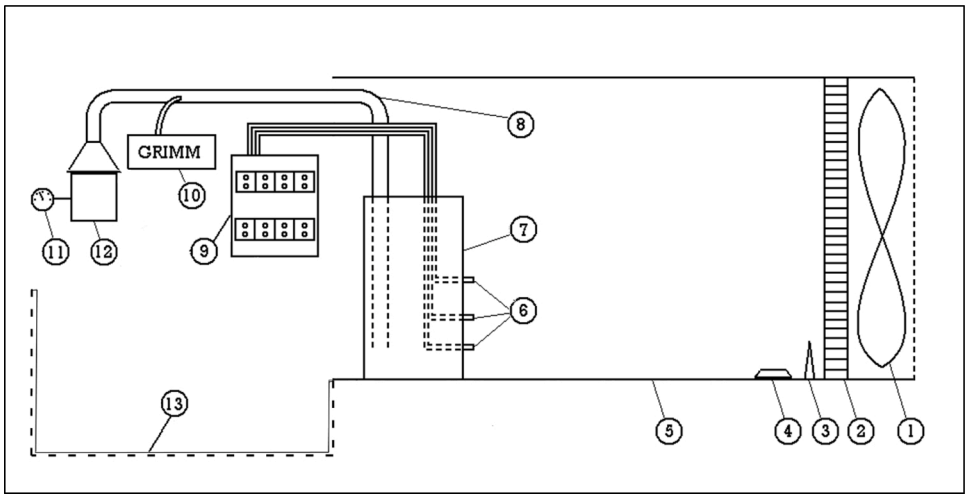

Fig. 1. Diagram of wind tunnel components and instrumentation for the tests (not drawn to scale). Components shown are: 1) fan, 2) honeycomb, 3) spires, 4) saltation source, 5) plywood floor, 6) static pressure pitot tubes, 7) particle sampler inlet, 8) dust sampling duct tube (63.5 mm ID), 9) pressure transducers, 10) Grimm particle sampler, 11) pressure gauge, 12) flow controller blower, and 13) saltation collection enclosure. Components 6-12 represent the isokinetic slot sampler system components.

dust monitor (Fig. 1, No. 10 - Model 1.108, Grimm Aerosol Technik GmbH & Co, Ainring, Germany) collecting mass flux samples in the collection pipe. Li et al. (2015) determined that PM10 as measured by the Grimm to be highly correlated ($R^2 = 0.990$) with that collected with a Hi-Vol sampling system (US-EPA reference method: RFPS-1287−063; Graseby Andersen, GMW Model 1200 High-Volume Air Sampler) using the same wind tunnel and sampling system as this study. Since the Grimm provided additional real-time measurement of PM2.5, the PM2.5 and PM10 results in this study are from Grimm measurements as were those in the previous two studies. All tests were conducted at the same wind speed of 13 m s^{-1}, which was the same speed as the previous studies in this series.

An enclosure (Fig. 1, No. 13) at the end of the tunnel consisted of a 2.4 H × 5.2 l × 1.4 W m chain-link fence with vertical plastic slats and was used to collect saltating samples from each run. The entire enclosure was lined with a polyethelene tarp that covered the floor and the sides of the enclosure to 1.5 m H. The upper portion of the enclosure was open to the atmosphere to allow wind dispersal.

2.2. Experimental procedure

2.2.1. Soil and tunnel preparation

This study used the same 15 soils (Table 1) from throughout the United States that were used in the studies of Li et al. (2015) and Tatarko et al. (2020). Note that Soil #6 was used for preliminary tests and not reported here. See Li et al. (2015) for more information regarding the collection and preliminary analysis of soils. Of these 15 soils, ten were sampled in pairs at five locations, with each pair having either

Table 1
Description of soils sampled, modified from Li et al. (2015). "ID" refers to the soil sample site designation. Note that site 6 was used for preliminary testing and is not included in the data presented.

ID	Location	Latitude Longitude	Texture	Series Name (Symbol)	Classification	Management
1	Manhattan, KS	39 12.671 N 96 35.749W	Silt loam	Ivan (Iv)	Fine-silty, mixed, mesic Cumulic Hapludolls	Conventional tillage: fallow winter wheat stubble (20+ yrs)
2		39 12.686 N 96 35.750W	Silt loam			No-till: corn (20+ yrs)
3		39 12.942 N 96 35.870W	Silt loam	Smolan (Sm)	Fine, smectitic, mesic Pachic Argiustolls	Conventional tillage: fallow winter wheat stubble (15+ yrs)
4		39 12.946 N 96 35.825W	Silt loam			No-till: winter wheat-sorghum-soybean (15 yrs)
5		39 13.787N 96 34.803W	Silty clay Loam	Chase (Cs)	Fine, smectitic, mesic Aquertic Argiudolls	Conventional tillage: continuous winter wheat
7		39 8.733 N 96 38.031W	Loamy fine sand	Stonehouse (St)	Sandy, mixed, mesic Typic Udifluvents	Conventional tillage: Soybean fallow
8		39 8.732N 96 37.903W	Loamy fine sand			Conventional tillage: Soybean Stubble
9	Pullman, WA	46 46.713N 117 4.953W	Silt loam	Palouse (Pa)	Fine-silty, mixed, mesic Pachic Ultic Haploxerolls	Conventional tillage: winter wheat-spring wheat-garbonzo (14 yrs)
10			Silt loam			No-till: winter wheat-spring wheat-garbonzo (14 yrs)
11	Bushland, TX	35 10.837N 102 5.581W	Clay loam	Pullman (Pu)	Fine, mixed, thermic Torrertic Paleustolls	Conventional tillage: wheat-sorghum-fallow (30 yrs)
12		35 10.846N 102 5.611W	Clay loam			No-till: wheat-sorghum-fallow (30 yrs)
13	Belle Glade, FL	26 39.387N 80 37.882W	Muck	Pahokee (Ph)	Euic, hyperthermic Lithic Haplosaprists	Lettuce
14	Canal Point, FL	26 52.008N 80 37.405W	Muck	Torry (Tr)	Euic, hyperthermic Typic Haplosaprists	Sugar cane
15	Pierre, SD	44 3.025N 100 8.557 W	Clay	Promise (Pr)	Very-fine, smetitic, mesic Typic Haplustert	Conventional tillage: (20+ yrs); most recently winter wheat
16		44 3.794N 100 9.740W	Clay			No-till: (20+ yrs); most recently sunflower

conventional tillage (CT) or no-till (NT) management ranging from 14 to 30 years prior to sampling (see Table 1).

Approximately 6 kg of saltation-size soil aggregates (0.15 to 0.84 mm) were obtained by sieving air-dried source-material soil with a 762 mm dia. vibratory sieve (SWECO, Florence, Kentucky). The sieving procedure was designed to overcome the weak inter-aggregate forces, but not the intra-aggregate forces. In general, the large aggregates were found to be the weakest as well as subjected to the largest impact forces in the sieves (Mirzamostafa et al., 1998). Hence, most breakage during the sieving process occurs in aggregates generally above the saltation size. While sieving is not perfect, it is a standard method used to successfully size aggregates as small as −0.01 mm (Syvitski, 1991).

Before testing each soil, the tunnel was swept with a broom and cleaned with compressed air to remove possible particulates retained in the tunnel. Also, the slot sampler system was tapped and cleaned with compressed air until spikes in the Grimm measurement were less than 100 μg m^{-3}. Before each saltation run, a background air concentration measurement (at least one-minute measurement) was ascertained using the Grimm.

2.2.2. Wind tunnel saltation tests

Each soil sample had three consecutive runs of saltation-size aggregates blown 12.4 m down the wind tunnel for a cumulative saltation distance of 37.2 m. The duration of each tunnel run was equal for all three consecutive runs and was determined by the amount of time needed during the first run for Grimm measurements to reach background concentrations plus one minute. After each run, the collection pipe was tapped with a small rubber mallet to dislodge any trapped particles as indicated by spikes in the Grimm measurements.

The initial saltation amount was weighed and placed in a 273 × 673 mm pile, 12.4 m upwind from the end of the tunnel floor (Fig. 1, No. 4). After each tunnel run, the amount of saltation retained in the enclosure area was weighed. The retained amount was used for the next tunnel run. A sub-sample (~100 g) was taken from the initial saltation-size aggregates as well as after each test run for moisture content correction. These moisture content samples were also used to determine sand content in the sample (see below, i.e., SF_{sand}). The test procedure described was replicated three times for each soil.

2.2.3. Determination of breakage parameters

FS_{sand} was determined by wet sieving of dispersed sub-samples collected in the enclosure at the end of the tunnel and horizontal saltation discharge in the form of primary sand particles (q_s) was determined from Eq 3. The results were used with Eq. 4 to calculate the coefficient of breakage (C_{bk}) and then used in Eq. 2 to calculate the vertical flux of suspension-size particles (Gss_{bk}) created during breakdown of saltating aggregates in the wind tunnel. PM2.5 and PM10 particle fluxes ($G2.5_{bk}$ and $G10_{bk}$ respectively) were measured by the Grimm dust monitor. The PM2.5 and PM10 fraction of suspension-size aggregates ($SF2.5_{bk}$ and $SF10_{bk}$, respectively) created during wind tunnel tests of saltation-size aggregates were calculated from Eqs. 5 and 6. The fraction of PM10 contributed by PM2.5 (i.e., the PM2.5/PM10 ratio) as a result of breakage were also calculated as the ratio of $SF2.5_{bk}$/$SF10_{bk}$. This ratio is used in the WEPS model to predict the amount of PM2.5 given the calculated amount of PM10.

2.3. Data analysis

Differences among soils in C_{bk}, and Gss_{bk} as well as $SF2.5_{bk}$ and $SF10_{bk}$ were determined by one-way analysis of variance (ANOVA) using the SPSS Statistics software package, Version 17.0. Multiple comparisons were made using Duncan's multiple-range test in Microsoft Excel. For statistical analysis of parameters, each of the three wind tunnel tests for each soil were considered as replicates of the breakage tests. Paired t-tests were used to determine differences in management types (CT vs. NT). A 5 % level of significance ($p < 0.05$) was used for all cases.

3. Results and discussion

3.1. Soil properties

Table 2 provides the particle size and organic matter content of the soils tested. The soils include a wide range in dispersed clay (4.4–82.7 %), silt (15.7–75.8 %), sand (1.6–66.6 %), PM2.5 (4.5–54.7 %), and PM10 (5.3–66.3 %). Organic matter ranged from 0.7–64.0 %. Note that soils 13 and 14 are classified as Histosols with 64 and 25.3 % organic matter respectively, and therefore dispersed PM2.5 and PM10 were not determined for these soils. However, soil 14 had the highest measured clay sized particles, which were likely organic in nature. Considering mineral dominated soils only (i.e., excluding soils 13 & 14), clay ranged from 4.4–52.2 %, silt from 29.1–75.8 %, and sand from 2.0 to 66.6 %. Organic matter content of the mineral soils ranged from 0.7 to 5.1 %.

Of the five soils paired as either CT or NT, three soils with CT management had higher sand (i.e., Sm, Pa, & Pr) while one (Pu) had the same sand content as that soil with NT management. For the Iv soil, NT management had lower sand content than the corresponding CT soil. In contrast, silt content of CT soils was lower for four of the five soil pairs (i.e., Iv, Sm, Pa, & Pu) than the same soils under NT management. In addition, four CT managed soils had lower organic matter contents (i.e., Iv, Sm, Pa, & Pu) than the same soil with NT management.

Recalling that all of the paired soils were under long term CT and NT management, it has been long recognized that vegetative cover reduces wind erosion (Chepil et al., 1963). These results support research showing that wind erosion can result in selective removal of silt and organic matter on sparsely vegetated soils (Lyles et al., 1985; Mirzamostafa et al., 1998) and that long term exposure of soils to wind erosion can reduce silt and organic matter content (Lyles and Tatarko, 1986).

3.2. Coefficient of breakage and suspension-size emissions

The C_{bk} and Gss_{bk} values for the 15 tested soils are presented in Table 3. C_{bk} values for all soils ranged from 0.004 (soil 16) to 0.069 m^{-1} (soil 8) and averaged 0.0163 m^{-1}. The lower the C_{bk} value, the stronger the aggregates and the more resistant they are to breakage (Mirzamostafa et al., 1998). As would be expected, the soils with the highest sand content (soils 7 & 8) also had the largest C_{bk} and also the weakest aggregates (Tatarko et al., 2020). Hagen (2004) determined average relative C_{bk} values of 0.044 by impacting saltation-size aggregates on a steel plate while our C_{bk} values were nearly 1/3 of that value in wind tunnel tests. This supports a later comment by Hagen and Fox (2020) that breakage from impact on a mobile target (e.g., in a wind tunnel) is less likely than breakage from impact on immobile targets (e.g., on a steel plate). In addition, our average C_{bk} value was not significantly different ($p < 0.05$) from that reported for wind tunnel studies by Mirzamostafa et al. (1998) (i.e., $C_{bk} = 0.00715$ m^{-1}), who only tested four soils from Kansas using smaller aggregates of 0.15 to 0.42 mm in diameter. Tatarko et al. (2020), using the same soils as the current study, reported abrasion coefficients of larger soil clods of 0.0543 m^{-1}, which is 3.4 times the average breakage coefficient of 0.016 m^{-1} reported in Table 3. Saltation-size aggregates were also found by Mirzamostafa et al. (1998) to be more stable than larger surface clods.

We assumed the findings of Mirzamostafa et al. (1998) who showed that C_{bk} was constant with the distance traveled down the wind tunnel floor. In addition, they found that C_{bk} varied with clay content. Similar to Mirzamostafa et al. (1998) we found C_{bk} to be inversely related to the percent clay in the soil (Fig. 2). For all soils in this study, including organic matter dominated soils (i.e., soils 13 & 14 with organic matter > 25 %), the relationship produced an $R^2 = 0.546$ (Fig. 2a). Given the unique properties of organic dominated soils and that particle size analysis of the soils with high organic matter content could inflate the reported clay content, we also determined the relationship of C_{bk} to clay content for mineral dominated soils (i.e., ≤ 5.1 % organic matter), which improved the fit and raised the R^2 to 0.818 (Fig. 2b).

Table 2
Particle size distribution and organic matter content of the study soils, modified from Li et al. (2015). Note that no dispersed PM was measured for the soils with high organic content (13 and 14).

			Dispersed Particle Size								
			PM2.5	PM10	PM2.5/PM10	Clay	Silt	Sand	Fine Sand	Very Fine Sand	Organic Matter
ID	Soil[a]	Tillage[b]	(%)	(%)		(%)	(%)	(%)	(%)	(%)	(%)
1	Iv	CT	21.3	30.9	0.690	20.6	74.4	5.0	0.4	4.5	3.0
2	Iv	NT	13.3	18.6	0.714	13.0	75.8	11.2	1.2	9.5	3.8
3	Sm	CT	31.2	38.1	0.819	30.5	63.9	5.5	0.5	4.8	2.9
4	Sm	NT	28.0	35.5	0.790	27.5	67.7	4.8	0.5	3.7	4.1
5	Cs	CT	26.9	36.4	0.740	26.4	70.9	2.7	0.2	2.3	2.8
7	St	CT	4.5	5.3	0.842	4.4	29.1	66.6	10.7	54.0	0.7
8	St	CT	7.3	9.4	0.780	7.1	56.8	36.1	5.0	28.9	1.7
9	Pa	CT	20.8	31.9	0.654	20.0	73.0	7.0	0.6	5.9	3.8
10	Pa	NT	21.1	32.3	0.655	20.0	73.7	6.3	0.7	4.9	5.1
11	Pu	CT	34.7	42.8	0.810	33.9	51.7	14.4	1.8	12.4	2.0
12	Pu	NT	32.2	40.2	0.801	31.5	54.1	14.4	1.7	12.6	2.3
13	Ph	CT	–	–	–	18.9	63.3	17.8	5.8	8.4	64.0
14	Tr	CT	–	–	–	82.7	15.7	1.6	0.8	0.6	25.3
15	Pr	CT	51.0	61.5	0.829	48.4	49.5	2.1	0.2	1.6	4.8
16	Pr	NT	54.7	66.3	0.826	52.2	45.8	2.0	0.3	1.1	4.4

[a] Soil refers to the Soil Symbol in Table 1.
[b] Tillage management where CT = Conventional tillage; NT = No-till.

Table 3
Measured mean coefficient of breakage (C_{bk}) and vertical flux of suspension-size aggregates from breakage of saltation-size aggregates (Gss_{bk}).

ID	Soil[a]	Tillage[b]	C_{bk} (m^{-1})		Gss_{bk} (kg m^{-2} s^{-1})	
			Average	Standard Deviation	Average	Standard Deviation
1	Iv	CT	0.009 def	0.001	0.091 b	0.021
2	Iv	NT	0.021 c	0.006	0.095 b	0.012
3	Sm	CT	0.010 def	0.001	0.094 b	0.016
4	Sm	NT	0.007 ef	0.001	0.049 b	0.011
5	Cs	CT	0.008 def	0.002	0.064 b	0.022
7	St	CT	0.036 b	0.015	0.074 b	0.072
8	St	CT	0.069 a	0.002	0.234 a	0.195
9	Pa	CT	0.012 def	0.001	0.062 b	0.017
10	Pa	NT	0.017 cd	0.002	0.081 b	0.019
11	Pu	CT	0.010 def	0.003	0.068 b	0.030
12	Pu	NT	0.007 ef	0.001	0.042 b	0.007
13	Ph	CT	0.012 def	0.006	0.052 b	0.015
14	Tr	CT	0.014 cde	0.001	0.059 b	0.038
15	Pr	CT	0.008 def	0.001	0.069 b	0.014
16	Pr	NT	0.004 f	0.002	0.036 b	0.012
Average			0.0163		0.0779	

Values with the same letter within a column are not significantly different between soil IDs ($p < 0.05$ level).
[a] Soil refers to the Soil Symbol in Table 1.
[b] Tillage management where CT = Conventional tillage; NT = No-till.

The suspension-sized flux from breakage (Gss_{bk}) ranged from 0.036 (soil 16) to 0.234 kg m^{-2} s^{-1} (soil 8) and averaged 0.0779 kg m^{-2} s^{-1}. Note that no soil was significantly different from the others ($p < 0.05$) except for soil 8, which had the greatest standard deviation of the measurements but also had the significantly greatest C_{bk} value. The study of Tatarko et al. (2020) also found abrasion coefficients and abrasion emissions from the same sandy soils (soils 7 & 8) to be significantly greater than the other soils. Note that the saltation process simulated in the wind tunnel represents the classic, very erodible scenario of a dry, bare, smooth condition under a constant wind. In an actual field situation, such suspension flux would be moderated greatly by surface conditions such as soil moisture, as well as by trapping of eroding material by soil and vegetative roughness under variable winds.

Fig. 3 shows the effect of prior long-term (i.e., 14 to 30 years) CT and NT management on C_{bk} and Gss_{bk}. Management significantly affected C_{bk} for four of the five soil pairs ($p < 0.05$), with only the Pu soil showing no significant difference (Fig. 3, upper plot). The three soils with the highest clay content (i.e., Sm, Pu, & Pr) had lower C_{bk} values with NT compared to than CT management, implying that high clay and NT management, or both result in more resistant aggregates to breakage than CT managed soils. In contrast, the two soils with the lowest clay content exhibited lower C_{bk} values under CT management. Tatarko et al. (2020) speculated that since long-term CT management retains less residue cover, it exposes the soil to greater selective removal of finer soil particles by wind erosion over time as observed by Lyles and Tatarko (1986). Thus, NT managed soils with higher clay contents result in more stable saltation size aggregates. In addition, cropping management has been shown to have an effect on dry aggregate stability by moderating freeze-thaw and freeze-dry processes (Layton et al., 1993). However, the overall effects of past climate and specific cropping histories at each site sampled in this study were unaccounted for, but nonetheless could have affected C_{bk} values.

Soils from long-term NT management showed significantly less vertical flux of suspension from breakage during saltation (Gss_{bk}) than CT management for only two of the five paired soils (i.e., Fig. 3, lower plot - Sm and Pr). These same two soil pairs also had significantly lower C_{bk} values under NT management. The other three soils showed no differences in management for Gss_{bk}.

3.3. Soil fraction of PM2.5 and PM10 and the PM2.5/PM10 ratio from breakage

The average soil fraction of PM2.5 ($SF2.5_{bk}$) and PM10 ($SF10_{bk}$) in suspension from breakage of saltating aggregates as well as the PM2.5/PM10 ratio are shown in Table 4. $SF2.5_{bk}$ ranged from 0.0015 (soil 15) to 0.0179 (soil 10) and averaged 0.0061 for all soils. $SF10_{bk}$ ranged from 0.0041 (soil 15) to 0.065 (soil 10) and averaged 0.0212 for all soils. Soil 15 with the lowest $SF2.5_{bk}$ and $SF10_{bk}$ was second highest in measured clay content among the soils at 48.4 %, excluding the two organic dominated soils. Soil 10 which has the highest $SF2.5_{bk}$ and $SF10_{bk}$ also had the highest organic matter content at 5.1 %, among the mineral dominated soils. Soil 10 had only the fourth greatest C_{bk} of the15 soils tested, perhaps indicating other factors (e.g., relatively high silt content

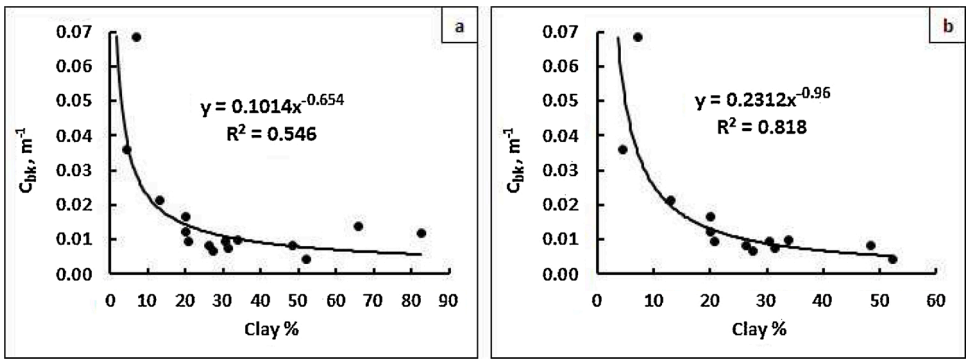

Fig. 2. The relationship of percent clay and coefficient of breakage (C_{bk}) for a) all soils tested and b) mineral soils only, with ≤ 5.1 % organic matter.

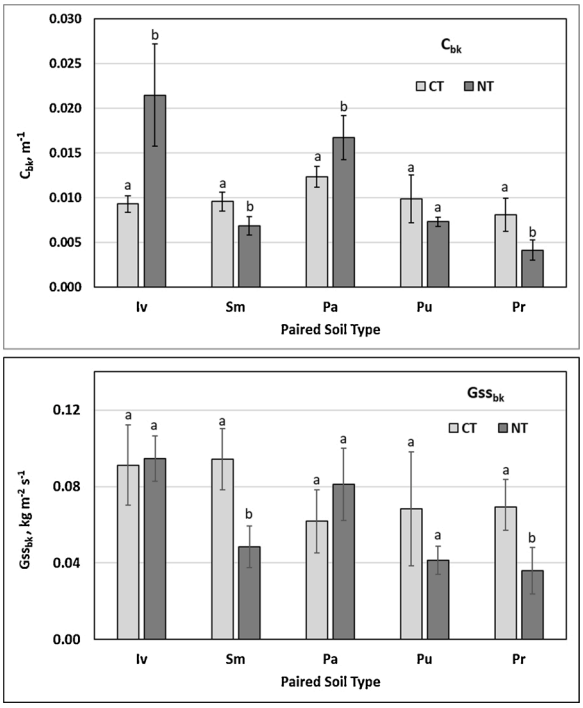

Fig. 3. Comparisons of coefficient of breakage (upper plot – C_{bk}) and vertical flux of suspension from breakage (lower plot – Gss_{bk}) for conventional tillage (CT) vs. no-tillage (NT) management on the same soils. Soils are Iv = Ivan (ID 1&2); Sm = Smolan (ID 3&4); Pa = Palouse (ID 9&10); Pu = Pullman (ID 11&12); and Pr = Promise (ID 15&16). Bars with the same letter are not significantly different ($p < 0.05$). Error bars represent one standard deviation.

at 73.7 %) contributed to its higher $SF2.5_{bk}$ and $SF10_{bk}$ values. Hagen (2004), in a chamber study reported that relative breakage increased with sand/clay ratio ($R^2 = 0.62$). We found no such relationship in our study, but we did see a better relationship between silt/clay and C_{bk} ($R^2 = 0.688$).

$SF2.5_{bk}$ values for soils 10 and 13 were significantly different from all other soils ($p < 0.05$). Soils 1, 9, and 13 as well as soil 10 were significantly different in $SF10_{bk}$ from all other soils. Soil 13 also had the highest organic matter content at 64 %. Previous studies on these same soils found the greatest PM2.5 and PM10 emission from the sandy soils (7 & 8) for loose emissions (Li et al., 2015) and abrasion emissions (Tatarko et al., 2020). The soil fraction of PM2.5 and PM10 from breakage did not follow a discernable pattern related to primary particle size in this study.

Four of the five soils paired by prior long-term management showed significant differences ($p < 0.05$) in breakage emissions in the form of $SF2.5_{bk}$ and $SF10_{bk}$ (Fig. 4). The three soils with the highest clay content (Pa, Pu, and Pr) also had significantly greater $SF2.5_{bk}$ and $SF10_{bk}$ under NT management, while the soil with the highest silt content (Iv) had significantly greater $SF2.5_{bk}$ and $SF10_{bk}$ under CT management. The fifth soil (Sm) showed no significant effect of prior management. Although the Sm-NT, Pu-NT and Pr-NT soils had lower C_{bk} values than the corresponding CT soils, indicating stronger aggregates of saltation size, the Pu-NT and Pr-NT soils nevertheless had a significantly greater fraction of PM2.5 and PM10 emitted compared to CT management. This simply indicates that for these two NT soils, the portion of the suspension emitted (Gss_{bk}) that was PM10 was greater than that of the corresponding CT soils, thus increasing the relative $SF2.5_{bk}$ and $SF10_{bk}$ values. We observed no relationship between $SF2.5_{bk}$ and $SF10_{bk}$ and primary particle size nor organic matter content that would explain why the PM10 fraction of suspension would be greater under NT compared to CT management. This unexpected behavior would suggest an area for further research.

Both the sources and the effects of fine particles (PM2.5) differ markedly from those of coarse particles (PM10) according to the US-EPA (1996). Thus it is beneficial to examine the relative contribution of PM2.5 and PM10 concentrations via the PM2.5/PM10 ratios. The PM2.5/PM10 ratios from breakage varied from 0.206 (soil 5) to 0.434 (soil 14) and averaged 0.2926 for all soils (Table 4). The two soils with the highest PM2.5/PM10 ratio were those dominated by high organic matter (soils 13 & 14), which were significantly different ($p < 0.05$) from the mineral dominated soils. The high organic soils (soils 13 & 14) also had significantly higher PM2.5/PM10 ratios ($p < 0.05$) than the mineral soils, suggesting that the PM2.5 organic matter was emitting at a greater rate than PM10. Similarly, Tatarko et al. (2020) found PM2.5/PM10 ratios for the same organic dominated soils to be greatest under abrasion of large clods (Tatarko et al., 2020). Of the mineral dominated soils, soil 7, which had the highest sand content as well as soils 15 and 16, which had the highest clay content, were collectively significantly different from the other soils. We also note that Hagen (2004) impacted saltation-size aggregates of the same size as this study from 9 states onto a steel plate in a chamber and found an average PM2.5/PM10 ratio from breakage to be 0.154, which is about one half of our average. He acknowledged that the chamber method would only provide relative breakage fractions and that absolute values could best be estimated by recycling soils in a wind tunnel.

The PM2.5/PM10 ratio is used in the WEPS model to predict PM2.5 given simulated PM10 (Hagen, 2004). Since the WEPS model already provides an estimate of PM10 from breakage, the approach used here was to determine the PM2.5 as a fraction of the PM10 (i.e., the PM2.5/PM10 ratio), which is the same approach used for loose and abrasion emissions in WEPS (Li et al., 2015; Tatarko et al., 2020). To predict the fraction of PM2.5 given PM10 in suspension under breakage as needed for the WEPS model, $SF2.5_{bk}$ vs. $SF10_{bk}$ were linearly plotted with the intercept set to zero (Fig. 5). Plot 5a included all soils in this study ($R^2 = 0.885$). Given the unique properties of organic dominated soils compared to mineral soils, plot 5b included only the mineral soils (excluding soils 13 & 4), which improved the linear fit ($R^2 = 0.972$). The

Table 4
Average soil fraction of PM2.5 ($SF2.5_{bk}$) and PM10 ($SF10_{bk}$) in suspension sized aggregates created during saltation breakdown, PM2.5/PM10 ratio, and standard deviations.

ID	Soil[a]	Tillage[b]	$SF2.5_{bk}$		$SF10_{bk}$		PM2.5/PM10	
			Average	Standard Deviation	Average	Standard Deviation	Average	Standard Deviation
1	Iv	CT	0.0086 bc	0.0011	0.0384 b	0.0046	0.224 ef	0.0090
2	Iv	NT	0.0047 def	0.0019	0.0197 c	0.0091	0.240 cdef	0.0100
3	Sm	CT	0.0035 ef	0.0005	0.0157 cde	0.0022	0.224 ef	0.0232
4	Sm	NT	0.0043 def	0.0005	0.0152 cde	0.0024	0.281 c	0.0155
5	Cs	CT	0.0028 ef	0.0006	0.0137 cdef	0.0027	0.206 f	0.0167
7	St	CT	0.0021 ef	0.0003	0.0060 ef	0.0005	0.343 b	0.0223
8	St	CT	0.0020 ef	0.0000	0.0082 def	0.0010	0.248 cdef	0.0299
9	Pa	CT	0.0104 b	0.0040	0.0354 b	0.0101	0.288 c	0.0293
10	Pa	NT	0.0179 a	0.0025	0.0648 a	0.0094	0.276 cd	0.0054
11	Pu	CT	0.0029 ef	0.0005	0.0126 cdef	0.0094	0.232 def	0.0507
12	Pu	NT	0.0052 de	0.0002	0.0199 c	0.0021	0.260 cde	0.0162
13	Ph	CT	0.0152 a	0.0030	0.0366 b	0.0101	0.423 a	0.0357
14	Tr	CT	0.0071 cd	0.0011	0.0164 cd	0.0027	0.434 a	0.0316
15	Pr	CT	0.0015 f	0.0004	0.0041 f	0.0013	0.375 b	0.0128
16	Pr	NT	0.0037 ef	0.0010	0.0107 cdef	0.0020	0.345 b	0.0372
Average			0.0061		0.0212		0.2926	

Values with the same letter within a column are not significantly different between soil IDs ($p < 0.05$ level).
[a] Soil refers to the Soil Symbol in Table 1.
[b] Tillage management where CT = Conventional tillage; NT = No-till.

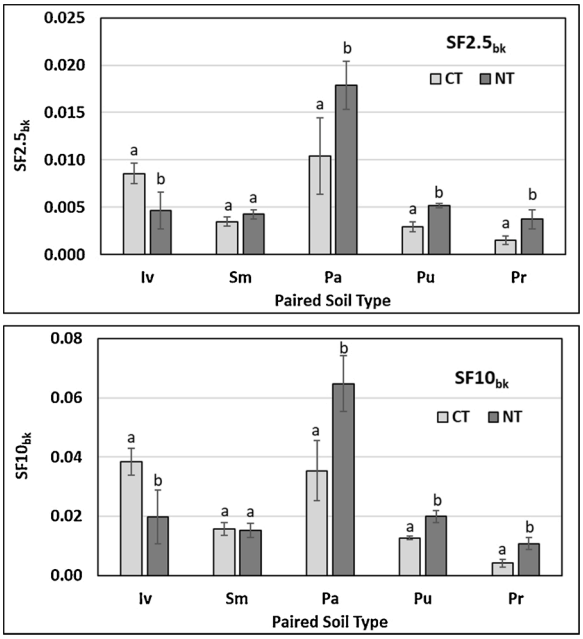

Fig. 4. Comparisons of soil in the form of PM2.5 (upper plot - $SF2.5_{bk}$) and PM10 (lower plot - $SF10_{bk}$) created during saltation breakage for no-tillage conventional tillage (CT) vs. No-Tillage (NT) management on the same soils. Soils are Iv = Ivan (ID 1&2); Sm = Smolan (ID 3&4); Pa = Palouse (ID 9&10); Pu = Pullman (ID 11&12); and Pr = Promise (ID 15&16). Bars with the same letter are not significantly different ($p < 0.05$). Error bars represent one standard deviation.

two points farthest above the line in Fig. 5a are the organic dominated soils (13 & 14) with the greatest PM2.5/PM10 ratios.

The resulting slope of the line under saltation breakage for mineral dominated soils is 0.2648, which provides the fraction of PM2.5 given the PM10 for WEPS simulation of PM2.5. The fraction determined for loose emissions by Li et al. (2015) was 0.1998 and for abrasions emissions by Tatarko et al. (2020), the fraction was 0.1693 as determined on these same soils. Thus this study shows that PM2.5 and PM10 emissions by breakage during saltation is the greatest of the three sources of emissions under wind erosion. Averaging the fractions from each source shows that overall, PM2.5 contributes 21.13 % of the PM10 generated by wind erosion for the soils studied. However, individual process effects on total emissions may vary. For example, loose emissions of suspension size material may be supply limited, and the contributions from that process will diminish accordingly.

4. Conclusions

Dust emission parameters from breakage under saltation were measured in a wind tunnel. The C_{bk} values determined were found to vary inversely with clay content and the relationship improved markedly when high organic soils were not included in the regression. This improvement is possibly because organic dominated soils have unique properties that govern their fine dust emission under breakage. No soil was found to be significantly different from the others in Gss_{bk} except one, which also had the significantly greatest C_{bk}. There were indications that $SF2.5_{bk}$ and $SF10_{bk}$ values are affected by clay and organic matter content but a clear relationship was not found. Management significantly affected C_{bk} for four of the five soil pairs, with the three soils with the highest clay, having lower C_{bk} values. Soils from long-term NT management showed significantly less vertical flux of suspension from breakage during saltation (Gss_{bk}) than CT management for only two of the five paired soils. A strong linear relationship was found for PM2.5 given PM10 under breakage that can be used in the WEPS model.

This research includes the only known study of PM2.5 generated under saltation breakage in a wind tunnel (i.e., not chamber studies). The results will further the knowledge of this important process that affects fine particulate emissions and will allow improved modeling of this dust fraction that affects air quality and health. It also supports previous research showing the importance of no-till and possibly other reduced tillage management on soil erosion reduction. Additional research is needed to determine the relationships of underlying soil properties as they affect emissions. Particularly, there is a need for a better understanding of the effects of organic dominated soils (i.e., Histosols) on the breakage process. In addition, the effects of cropping and weather history on the variability of breakage emissions is indicated. Further studies to determine potential changes in particle size distribution and organic matter resulting from breakage of saltating soil aggregates are also warranted.

This research furthers our knowledge of fine dust emissions from breakage of saltating aggregates in the wind. In particular, this study advances our understanding of the generation of PM2.5 and PM10 that are known health hazards. It also provides parameters that can be used

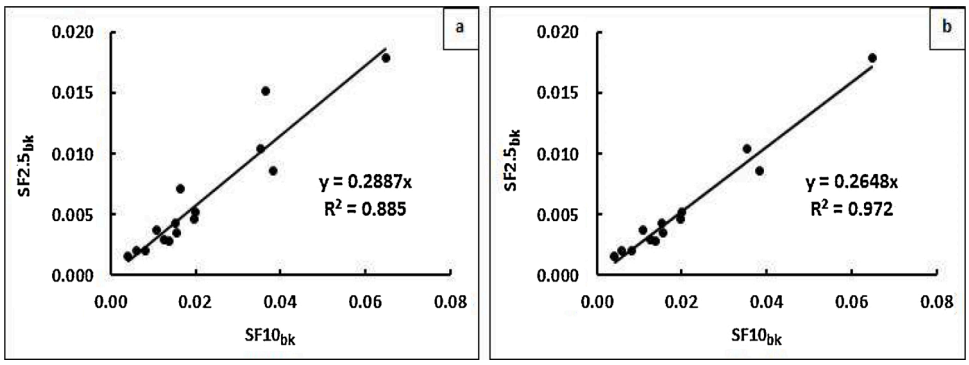

Fig. 5. The relationship of $SF2.5_{bk}$ to $SF10_{bk}$ for all soils tested (a) and mineral soils only with organic matter content < 25 % (b). The slope of each regression represents the predicted PM2.5 given PM10.

in wind erosion modeling efforts such as the WEPS model. More refined wind erosion models will allow for more accurate erosion assessments and effective controls for improved air quality.

Disclaimer

Mention of trade names or commercial products is solely for the purpose of providing specific information and does not imply recommendation or endorsement by the U.S. Department of Agriculture. The USDA is an equal opportunity provider and employer.

Declaration of Competing Interest

The authors declare that they have no known competing financial interests or personal relationships that could have appeared to influence the work reported in this paper.

References

Chenglai, W., Liu, X., Lin, Z., Rahimi-Esfarjani, S.R., Lu, Z., 2018. Impacts of absorbing aerosol deposition on snowpack and hydrologic cycle in the Rocky Mountain region based on variable-resolution CESM (VR-CESM) simulations. Atmos. Chem. Phys. 18, 511–533. https://doi.org/10.5194/acp-18-511-2018.

Chepil, W.S., Woodruff, N.P., Siddoway, F.H., Fryrear, D.W., Armbrust, D.V., 1963. Vegetative and nonvegetative materials to control wind and water erosion. Soil Sci. Soc. Am. Proc. 27 (1), 86–89.

Dockery, D.W., Pope 3rd., C.A., Xu, X., Spengler, J.D., Ware, J.H., Fay, M.E., Ferris Jr., B. G., Speizer, F.E., 1993. An association between air pollution and mortality in six U.S. Cities. N. Engl. J. Med. 329, 1753–1759. https://doi.org/10.1056/NEJM199312093292401pmid:8179653.

Goudie, A.S., 2014. Desert dust and human health disorders. Environ. Int. 63, 101–113. https://doi.org/10.1016/j.envint.2013.10.011.

Hagen, L.J., 2004. Fine particulates (PM10 and PM 2.5) generated by breakage of mobile aggregates during simulated wind erosion. Trans. ASAE 47 (1), 107–112.

Hagen, L.J., Fox, F.A., 2020. Erosion submodel of WEPS. In: Tatarko, J. (Ed.), The Wind Erosion Prediction System (WEPS): Technical Documentation. USDA Agriculture Handbook 727:84-157. United States Department of Agriculture, Agricultural Research Service, Beltsville, MD. Available in digital only at the National Agricultural Library Digital Collections. https://naldc.nal.usda.gov/catalog/7105679).

Karlen, D.L., Wollenhaupt, N.C., Erbach, D.C., Berry, E.C., Swan, J.B., Eash, N.S., Jordahl, J.L., 1994. Crop residue effects on soil quality following 10-years of no-till corn. Soil Tillage Res. 31, 149–167. https://doi.org/10.1016/0167-1987(94)90077-9.

Kjelgaard, J.F., Chandler, D.G., Saxton, K.E., 2004. Evidence for direct suspension of loessial soils on the Columbia Plateau. Earth Surf. Process. Land. 29, 221–236. https://doi.org/10.1002/esp.1028.

Lambert, F., Delmonte, B., Petit, J.R., Bigler, M., Kaufmann, P.R., Hutterli, M.A., Stocker, T.F., Ruth, U., Steffensen, J.P., Maggi, V., 2008. Dust - climate couplings over the past 800,000 years from the EPICA Dome C ice core. Nature 452, 616–619. https://doi.org/10.1038/nature06763.

Layton, J.B., Skidmore, E.L., Thompson, C.A., 1993. Winter-associated changes in dry-soil aggregation as influenced by management. Soil Sci. Soc. Am. J. 57, 1568–1572.

Li, H., Tatarko, J., Kucharski, M., Dong, Z., 2015. PM2.5 and PM10 emission from agricultural soils by wind erosion. Aeolian Res. 19, 171–182. https://doi.org/10.1016/j.aeolia.2015.02.003.

Li, J., Kandakji, T., Lee, J.A., Tatarko, J., Blackwell, J., Gill, T.E., Collins, J.D., 2017. Blowing dust and highway safety in the southwestern United States: characteristics of dust emission "hotspots" and management implications. Sci. Tot. Environ. 621, 1023–1032. https://doi.org/10.1016/j.scitotenv.2017.10.124.

Liu, C., et al., 2019. Ambient particulate air pollution and daily mortality in 652 cities. N. Engl. J. Med. 381, 705–715. https://doi.org/10.1056/NEJMoa1817364pmid:31433918.

Lopez, M.V., Garcia, R., Arrue, J.L., 2000. Effects of reduced tillage on soil surface properties affecting wind erosion in semiarid fallow lands of Central Aragon. Eur. J. Agron. 12, 191–199.

Lyles, L., Tatarko, J., 1986. Wind erosion effects on soil texture and organic matter. J. Soil Water Conserv. 41 (3), 191–193.

Lyles, L., Cole, G.W., Hagen, L.J., 1985. Wind erosion: processes and prediction. In: Follett, R.F., Stewart, B.A. (Eds.), Soil Erosion and Crop Productivity. Wisconsin, Madison, pp. 163–172. Chapt. 10.

Middleton, N.J., 2017. Desert dust hazards: a global review. Aeolian Res. 24, 53–63.

Mirzamostafa, N., 1996. Suspension Component of Wind Erosion. Ph.D. Diss. Kansas State Univ., Manhattan (Diss. Ahstr. 9714341).

Mirzamostafa, N., Hagen, L.J., Stone, L.L., Skidmore, E.L., 1998. Soil aggregate and texture effects on suspension components from wind erosion. Soil Sci. Soc. Am. J. 62, 1351–1361.

Painter, T.H., Skiles, S.M.K., Deems, J.S., Bryant, A.C., Landry, C.C., 2012. Dust radiative forcing in snow of the Upper Colorado River Basin: 1. A 6 year record of energy balance, radiation, and dust concentrations. Water Resour. Res. 48, 1–14. https://doi.org/10.1029/2012WR011985.

Painter, T.H., Skiles, S.M., Deems, J.S., Brandt, W.T., Dozier, J., 2017. Variation in rising limb of Colorado River snowmelt runoff hydrograph controlled by dust radiative forcing in snow. Geophys. Res. Lett. 44. https://doi.org/10.1002/2017GL075826.

Prospero, J.M., Lamb, P.J., 2003. African droughts and dust transport to the Caribbean: climate change implications. Science 302, 1024–1027. https://doi.org/10.1126/science.1089915.

Sheehy, J., Regina, K., Alakukku, L., Six, J., 2015. Impact of no-till and reduced tillage on aggregation and aggregate-associated carbon in Northern European agroecosystems. Soil Tillage Res. 150, 107–113. https://doi.org/10.1016/j.still.2015.01.015.

Skidmore, E.L., Layton, J.B., Armbrust, D.V., Hooker, M.L., 1986. Soil physical properties as influenced by cropping and residue management. Soil Sci. Soc. Am. J. 50 (2), 405–419.

Syvitski, J.P., 1991. Principles, Methods, and Application of Particle Size Analysis. Cambridge Univ. Press, New York.

Tatarko, J., Wagner, L., Fox, F., 2019. The Wind Erosion Prediction System and its use in conservation planning. In: Wendroth, O., Lascano, R.J., Ma, L. (Eds.), Bridging Among Disciplines by Synthesizing Soil and Plant Processes. Adv. Agric. Syst. Model. 8:71-101. ASA, CSSA, and SSSA, Madison, WI.

Tatarko, J., Kucharski, M., Li, H., Li, H., 2020. PM2.5 and PM10 emissions by abrasion of agricultural soils. Soil Tillage Res. 200, 104601 https://doi.org/10.1016/j.still.2020.104601.

US Federal Register, 2013. National Ambient Air Quality Standards for Particulate Matter; Final Rule. Register 40 CFR Part 58.

US-EPA, 1996. Air Quality Criteria for Particulate Matter Volume I of III. Environ. Prot. I, p. 178.

US-EPA, 1999. Compendium of Methods for the Determination of Inorganic Compounds in Ambient Air. EPA/625/R-96/010a, Cincinnati, OH.

Van Pelt, R.S., Zobeck, T.M., Baddock, M.C., Cox, J.J., 2010. Design, construction, and calibration of a portable boundary layer wind tunnel for field use. Trans. ASABE. 53 (5), 1413–1422.

Wagner, L.E., 2013. A history of wind erosion models in the United States Department of Agriculture: the Wind Erosion Prediction System (WEPS). Aeolian Res. 10, 9–24. https://doi.org/10.1016/j.aeolia.2012.10.001.